Connal Luke (Orcid ID: 0000-0001-7519-977X)

Temperature-induced self-assembly and metal ion-stabilization of histidine functional block copolymers

Emma R. L. Brisson,[a] James C. Griffith,[b] Ayana Bhaskaran,[c] George V. Franks,[a] Luke A. Connal*[c]

[a] Department of Chemical Engineering and Particulate Fluids Processing Centre, The University of Melbourne, Parkville, Victoria 3010, Australia.

[b] Materials Characterisation and Fabrication Platform, University of Melbourne, Parkville, Melbourne 3010, Australia.

[c] Research School of Chemistry, Australian National University, Canberra, Australian Capital Territory 2601, Australia.

Email: luke.connal@anu.edu.au

Abstract

Histidine functional block copolymers are thermally self-assembled into polymer micelles with poly-*N*-isopropylacrylamide in the core and the histidine functionality in the corona. The thermally induced self-assemblies are reversible until treated with Cu^{2+} ions at 50 °C. Upon treatment with 0.5 equivalents of Cu^{2+} relative to the histidine moieties, metal ion coordination locks the self-assemblies. The self-assembly behavior of histidine functional block copolymers is explored at different pH using dynamic light scattering and ^{1}H NMR. The metal ion coordination locking of the histidine functional micelles is also explored at different pH values, with stable micelles forming at pH 9, observed by dynamic light scattering and imaged by atomic force microscopy. The thermal self-assembly of glycine functional block copolymers at pH 5, 7 and 9 are similar to the histidine functional materials, however the self-assemblies do not become stable after the addition of Cu^{2+}, indicating that the imidazole plays a crucial role in the metal ion coordination that locks the micelles. The reversibility of the histidine-copper complex locking mechanism is demonstrated by the addition of acid to protonate the imidazole and destabilize the polymer self-assemblies.

This is the author manuscript accepted for publication and has undergone full peer review but has not been through the copyediting, typesetting, pagination and proofreading process, which may lead to differences between this version and the Version of Record. Please cite this article as doi: 10.1002/pola.29351

Keywords

histidine, metal ion coordination, self-assembly, thermal response, reductive amination

Introduction

The self-assembly of block copolymers is a promising area of polymer chemistry and engineering with technological applications in drug and vaccine delivery,[1–3] sensing,[4,5] catalysis,[6,7] and more. The self-assembly of block copolymers depends on many factors, including polymer architecture, amphiphilicity, polymer moleculear weights and polymer functionality.[8,9] Some polymers can change their properties in response to a stimulus, including pH, temperature, light, electrolytes, and others, classifying them as 'smart' materials.[10,11] The incorporation of smart materials into block copolymers enables stimuli-responsive block copolymer assembly or disassembly, as well as the ability to tune the chemical composition of the micelles. The functionality of polymers included in block copolymer designs can play very important roles in the application of the polymer self-assemblies. For example, the reversible conjugation of drugs to the polymer corona can be used for targeted load delivery. The incorporation of fluorine atoms into certain blocks of block copolymers can enable their use as MRI contrast agents.[12–14] and also enable sensing capabilities.[5] The mechanism of drug or gene delivery can also be the disassembly of the polymer micelles upon exposure to a certain stimulus, such as a change in pH.[3,15,16]

In addition to the tailoring of block copolymers for specific applications, polymer functionality can be used to lock micelles into their self-assembled structures in addition to reversible assemblies. As polymer self-assemblies are dynamic in nature, their stability can be compromized at elevated temperature, low concentrations, or in turbulent conditions.[17] Permanently stabilizing polymer self-assemblies has been achieved by using covalent chemistries either in the core or the corona of the self-assembly, in addition to the chain ends. In some applications, it is acceptable to lock the polymer self-assemblies permanently, however the ability to manipulate the self-assemblies based on external stimuli is a highly attractive reason to instead employ dynamic cross-linking strategies. The use of responsive and highly functional building blocks to make block copolymers allows for their assembly and disassembly,[18] in addition to their changing shapes or sizes based on external stimuli.[11,19,20] It has been demonstrated that polymer micelles are more readily uptaken into cells than their unimers,[21] and as a result, acid degradable polymers have been a focus in polymer cancer therapy

developments.[15,22] In addition to pH as a stimulus, polyelectrolytes have been used to reversibly lock micelles using electrostatic interactions and electrolytes as stimuli.[23] Other dynamic chemistries have been employed in zwitterionic polymers, coascervates,[24] disulphide exchange chemistry,[25] carbon dioxide,[26] and Diels-Alder chemistry.[27] The ability to dynamically lock micelles into place with a wide range of chemistries and interactions is important to further develop block copolymer based technologies.[28]

Our group has a large focus on biomimicry, and part of that comes with a focus on the synthesis of amino acid functional polymers. Amino acids are highly functional moieties with an amine, a carboxylic acid and an R-group, which can have hydrophobic, polar, acidic or basic functionalities.[29] One amino acid of particular interest to our group for application in material science has been histidine. Histidine has important roles in both catalysis[30] as well as in metal ion coordination.[31] Histidine mimicking materials have been used in metal ion coordination gels,[32–35] as well as in pH responsive gels.[36] The pH response of histidine is also highly physiologically relevant. It is protonated below pH 7 and deprotonated above. Its pH responsive nature has let it be used as a pH responsive destabilization system.[37] Histidine has the advantage of being a naturally occurring, important ligand for divalent metals.[32] The use of metal ion coordination as a dynamic bond is widely studied in self-healing materials and in templated materials, however the application to block copolymer self-assembly has been limited. Van der Gucht and coworkers used chelideamic acid functional polymers and used zinc ions to induce micellization of amphiphilic block copolymers.[38] Liu et al has made ruthenium core crosslinked metal ion micelles, as well as some magnetic metal containing micelles. [39] [40] Jäkle has done nice supramolecular self-assembly work using metal ion coordination of polymer supported tris(2-pyridyl)- borates, however it is not demonstrated to be reversible and the structures are micron sized.[41] Zhuo et al stabilized micelles using metal ion coordination of PEI with both copper and ruthenium and used these to synthesized Pt nanoparticles.[42,43] The incorporation of histidine as an important natural ligand for metal ion coordination into a block copolymer self-assembly is an exciting way to add some dynamic chemistry to the reversible locking of self-assemblies in the corona.

In this paper, we synthesize temperature-responsive, histidine functional block copolymers that can be reversibly locked using metal ion coordination using Cu^{2+} ions that coordinate to the histidine moieties; while divalent copper ions are toxic to cells, they are well known to coordinate strongly to histidine, making it a great choice to demonstrate this. The synthesis of our block copolymers via our

previously reported synthesis strategy using reductive amination expands the application of this post polymerization approach to aldehyde functional block copolymer architectures. The incorporation of a PNiPAm block allows for reversible, temperature-responsive micellization. Upon the addition of Cu^{2+} at elevated temperatures, the temperature-responsiveness of the micelles is lost, as the micelles are locked into place and as demonstrated by measurements upon cooling. The effect of pH on the self-assembly, as well as the metal ion coordination of these materials is explored. The reversibility of the metal ion coordination on the micelle formation is demonstrated by the addition of acid, observed after swirling the solution for about ten seconds. The self-assembly and metal ion coordination of the polymers is compared to glycine functional polymers, to highlight the need for the imidazole group in the Cu^{2+} complexation.

Materials and Methods

Materials

Unless otherwise stated, chemicals were used as received. *N*-isopropylacrylamide (NiPAm; 98%, stabilized with MEHQ) was obtained from Tokyo Chemical Industry Co., Ltd., and recrystallized from a toluene:*n*-hexane mixture (2:3 by volume) prior to use. Azobis(isobutronitrile) (AIBN; 98%), 3-vinylbenzaldehyde (3VBA; 97%), cyanomethyl dodecyl trithiocarbonate (CDT; 98% by HPLC), glycine (ACS reagent, >98.5%), 1,4-dioxane (>99.0), dimethyl formamide (DMF, spectrometer grade), lithium bromide (LiBr; 99%), sodium acetate (>99.0%), cupric chloride (97%), TRIS (99.9%), and BIS TRIS (98%) were obtained from Sigma Aldrich. AIBN was recrystallized from cold methanol prior to use. L-histidine (98%), and sodium borohydride (98%) were manufactured by Alfa Aesar and obtained from VWR. Sodium hydroxide (>99%) was manufactured by Acros organics and obtained from VWR. Hydrochloric acid (1.0 M) and glacial acetic acid were manufactured by AjaxFineChem. Toluene (Analar Normapur) was purchased from VWR. Functionalized polymers were dialysed against double distilled water using dialysis tubing (regenerated cellulose, SnakeSkin™, 10000 MWCO) obtained from Life Technologies Australia. Diethyl ether (99%) and *n*-hexane (95%) were of RCI Premium grade from ACI Labscan. Methanol (MeOH; reagent grade) was manufactured by Chem-Supply. Buffers (sodium acetate:acetic acid pH 5, BIS TRIS pH 7, and TRIS HCl pH 9) were prepared at 0.6M and adjusted to the desired pH using 1.0 M HCl or NaOH solutions. These buffers were chosen because they are the same used by Fullenkamp and other in the synthesis of histidine-based metal ion coordination gels.[32]

Instrumentation

Proton nuclear magnetic resonance (^{1}H NMR) spectra were taken with a Varian 400 MHz spectrometer in the specified deuterated solvent. Size Exclusion Chromatography (SEC) was used to characterize the molecular weight of synthesized polymers. Samples were prepared by dissolving the polymer in spectrometry grade DMF at 5 mg mL^{-1} and filtering them through a 0.45 µm Teflon^{TM} filter prior to injection. 50 µL of sample solution was injected and flowed through the instrument columns and detectors at 1 mL min^{-1}. The SEC instrument, operating at 70 °C, was equipped with two Phenomenex Phenogel columns (5 µm bead size, 104 and 106 Å porosity) in series, a Shimadzu RID-10 refractometer (λ = 633 nm), and a Shimadzu SPD-20A UV-Vis detector. The mobile phase was 0.05M LiBr in DMF. The molecular weights of the polymers were determined by comparison to a calibration curve determined by known polystyrene standards. The pH of aqueous solutions were measured using a HACH SensION+ PH31 with a 5014 T probe. Dynamic Light Scattering (DLS) measurements were taken with a Wyatt DynaPro NanoStar DLS/SLS with a quartz cuvette after samples were filtered through a 0.45 µm Nylon^{TM} filter; complete histograms, correlation functions, and %PD are presented for each DLS data measurement presented in the SI. Atomic Force Microscopy (AFM) images were acquired using a Cypher S AFM (Oxford Instrument's Asylum Research, Santa Barbara, USA) operating in tapping mode in air. AFM samples were prepared by drop casting 10 µl of solution (0.5 mg ml^{-1}) onto 1x1 cm^2 silicon wafer pieces then allowing them to air dry in a laminar flow hood before transferring to the AFM sample stage. BlueDrive photothermal excitation was used to actuate AC240TS-R3 probes (Asylum Research, USA) mounted in a standard air holder. Spring constants of 1.7 – 2.6 N/m were recorded and resonance frequencies of 65 kHz – 80 kHz. Free air amplitudes of 650 mV were used for each probe and set points of 450 – 500 mV used to engage on the surface. Images were obtained at scan rates of 1 Hz and with 512 lines. WaveMetrics Igor Pro v6.35 and Asylum Research AFM Software v14 were used for image analysis.

Synthesis

Poly(N-isopropylacrylamide)$_{80}$ macro chain transfer agent (MCTA). Into a Schlenk tube equipped with a magnetic stir bar, NiPAm (6.010 g, 53.11 mmol), CDT (0.208 g, 0.65 mmol), and AIBN (0.011 g, 0.067 mmol) were added and dissolved in 1,4-dioxane (8.75 mL). The mixture was degassed using three freeze-pump-thaw cycles and with the vacuum released under argon atmosphere, and the Schlenk tube was immersed into an oil bath at 65 °C to begin polymerization. The polymerization was stopped after 2 hours 10 minutes. The MCTA was precipitated into diethyl ether twice and allowed to

air dry, yielding a pale yellow powder. **^{1}H NMR** (400 MHz, $CDCl_3$): δ = 7.3-5.8 (b, 76 H), 4.0 (bs, 80 H), 3.3 (bs, 2H), 2.5-0.9 (backbone, 761 H). **SEC** (DMF): M_n = 16800, M_w = 14400; Đ = 1.17.

Poly[(N-isopropylacrylamide)$_{80}$-*b*-(3-vinylbenzaldehyde)$_{27}$]. MCTA (0.5 g, 49 µmol), 3VBA (0.3988 g, 3.02 mmol) and AIBN (29 µL of a 1 mg mL^{-1} solution in 1,4-dioxane, 1.8 µmol) were dissolved into 1.0 mL 1,4-dioxane and added to a Schlenk tube equipped with a magnetic stir bar. The mixture was degassed by three freeze-pump-thaw cycles and the vacuum was released under argon atmosphere. The reaction was stopped after 6 hours and the polymer was precipitated into diethyl ether and allowed to air dry, yielding **P1** as a pale yellow powder. **^{1}H NMR** (400 MHz, $CDCl_3$): δ = 10.0-9.6 (bs, 27 H), 7.7-5.9 (b, 184 H), 4.0 (bs, 80 H), 2.4-0.9 (backbone, bm, 856 H). **SEC** (DMF): M_n = 27700, M_w = 22000; Đ = 1.27.

Poly[(N-isopropylacrylamide)$_{80}$-*b*-(3-vinylbenzaldehyde)-co-histidine$_{25}$] (**P_{HIS}**). Into a vial, histidine (1.4 eq 43.1 g, 0.278 mmol) was stirred in an equimolar solution of NaOH in MeOH (510 µL of a 0.5 M stock solution) until dissolved. **P1** (0.091 g, 0.195 mmol aldehyde) was added to the histidine solution and stirred for two hours. Sodium borohydride (4 eq, 25.6 mg, 0.779 mmol) was added and the solution was stirred at room temperature overnight. The methanol was evaporated and replaced with an equal volume of distilled water, and the polymer solution was dialysed against distilled water with at least three water changes. The water was removed by lyophilization, yielding a fluffy white powder. **^{1}H NMR** (400 MHz, CD_3OD): δ = 8.2-6.1 (bs, 111 H), 4.4 (b, 4 H), 4.8 (bs, 101 H), 3.6 (bs, 12 H), 3.1 (bs, 21 H) 2.5-1 (backbone, bm, 801 H).

P_{GLY} was synthesized in the same manner as **P_{HIS}**, with glycine substituted for histidine. **^{1}H NMR** (400 MHz, $CDCl_3$): δ = 7.8-6.1 (bs, 79 H), 4.3-3.7 (bm, 108 H), 3.6-3.0 (bs, 35 H), 2.5-0.7 (backbone, bm, 801 H).

Temperature-responsive micelles. Polymer solutions with a concentration of 0.5 mg mL^{-1} of polymer in 0.1 M buffer solutions were prepared and filtered through 0.22 µm Nylon™ filters. To measure the polymer behavior above and below the LCST of the PNIPAM block were investigated by taking DLS measurements of the polymers solutions at 25 °C, 50 °C and again at 25 °C after cooling. The polymer solutions were gently stirred and held at the measurement temperature for a minimum of 5 minutes before a measurement was taken. To study this by ^{1}H NMR, the polymer was dissolved into D_2O at a concentration of 20 mg mL^{-1} and the solution was heated in the spectrometer without stirring.

Copper locked micelles. To lock the micelles using metal ion coordination, cupric chloride was added to the gently stirring polymer solutions after they had been heated at 50 °C for five minutes. After the addition of the Cu^{2+} ions, the polymer solutions were allowed to cool to room temperature with gentle stirring. Separately, the copper ions were also added at 25 °C, to ensure that the self-assembly was not driven by the coordination or by the addition of copper. In these samples, the copper was added to the stirring polymer solutions at 25 °C and subsequently heated to 50 °C for 5 minutes and once again cooled to 25 °C while stirring.

Results and discussion

The synthesis of histidine and glycine functional block copolymers was undertaken using the protecting group-free post-polymerization functionalization approach developed by our group, illustrated in Scheme 1.[44] To achieve this, an aldehyde containing block copolymer was synthesized. First, a temperature-responsive, PNiPAm, macro chain transfer agent (**MCTA**) was synthesized using RAFT polymerization. The degree of polymerization of the **MCTA** was determined to be 80 with good control over dispersity ($Đ$=1.17), confirmed by ^{1}H NMR, shown in in Figure 1a, and SEC in Figure S1. The **MCTA** was chain extended with 3-vinylbenzaldehyde (3VBA) to form the diblock copolymer **P1**, poly(N-isopropylacrylamide$_{80}$-*block*-3vinylbenzaldehyde$_{27}$), maintaining good control over the polymerization ($Đ$=1.27) by keeping the radical initiator concentration low. The incorporation of the aldehyde was determined by comparing the ^{1}H NMR signal from the aldehyde at δ 10 (peak *c* in Figure 1b) with the methine proton of the isopropyl group of the NiPAm moiety at δ 4 (*b*).

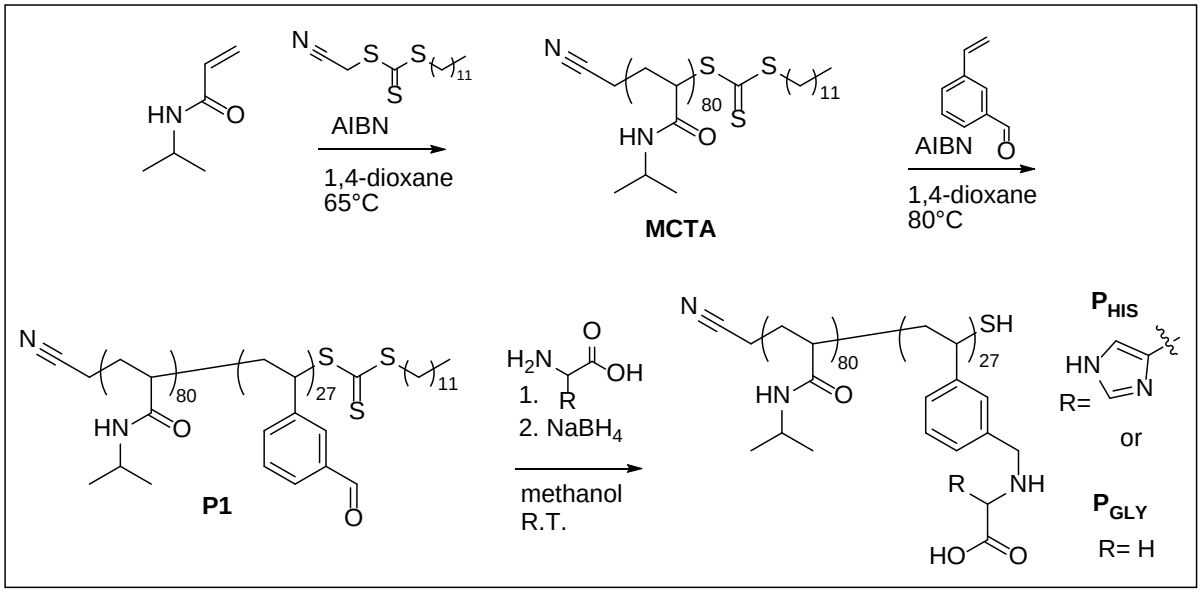

Scheme 1 A temperature-responsive, benzaldehyde functional diblock copolymer, **P1**, was synthesized by RAFT polymerization. A macro chain transfer agent (**MCTA**) was first synthesized from NiPAm which was subsequently chain extended with 3VBA. The post-polymerization functionalization of **P1** was performed using reductive amination with both glycine and histidine to form $\mathbf{P_{GLY}}$ and $\mathbf{P_{HIS}}$, respectively.

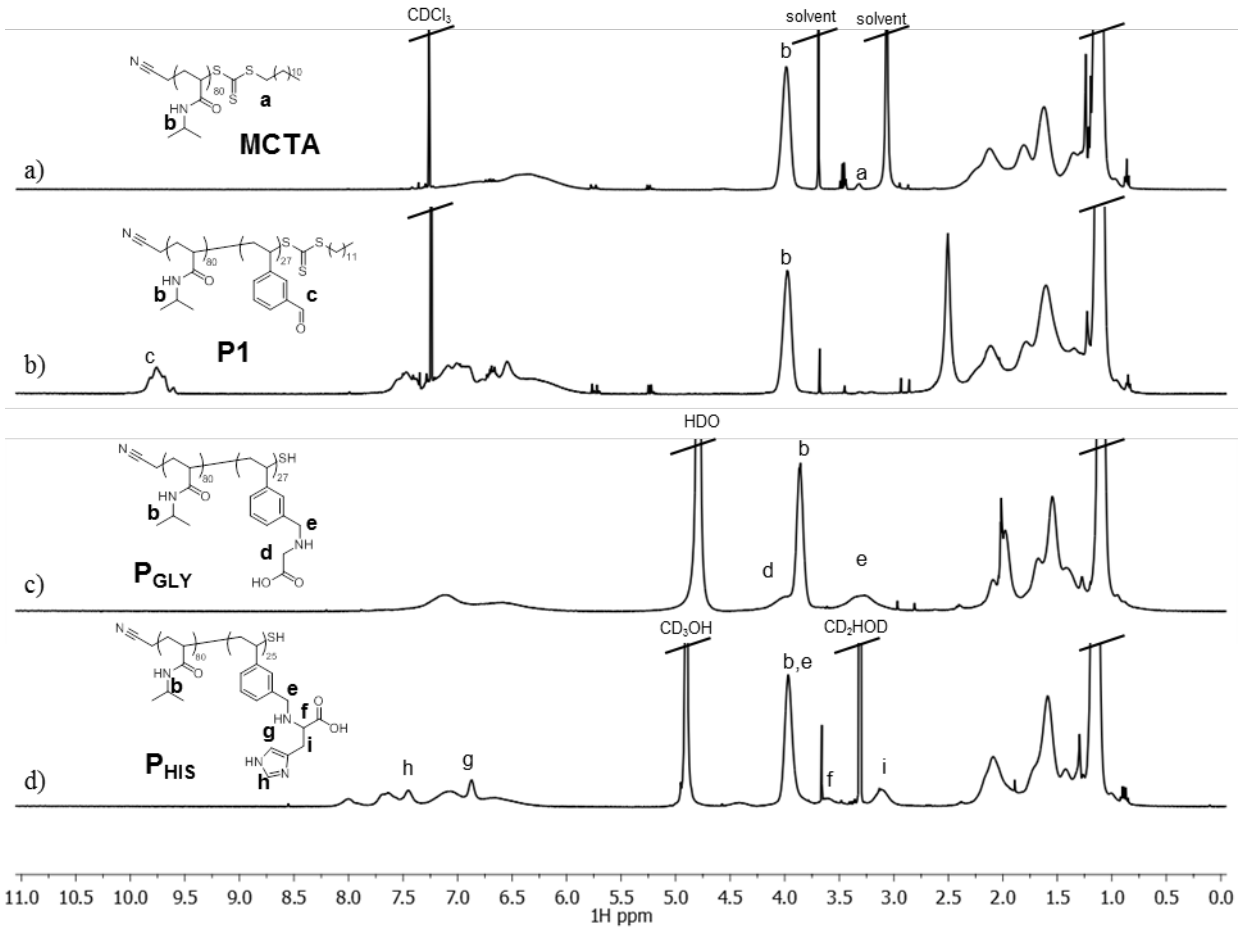

Fig. 1 The ^{1}H NMR spectra showing the synthesis and functionalization of the block copolymers: **MCTA** (a), **P1** (b), $\mathbf{P_{HIS}}$ (c) and $\mathbf{P_{GLY}}$ (d).

The diblock copolymer **P1** was functionalized with histidine and glycine using reductive amination. Initially, the amino acid with one equivalent of base in methanol was added to the polymer (**P1**) to form an imine. The imine bond was reduced to an amine using sodium borohydride. The aldehyde peak shown in Figure 1b (peak *c*) disappears after functionalization with glycine and histidine (Figures 1c and 1d respectively). The amount of glycine functionality achieved was 100%, within error of the NMR measurement, determined by comparing the backbone intensity to peaks *d* and *b*. The amount of histidine functionality achieved was 95%, within the error of the NMR measurement, determined by comparing the backbone protons to the two protons at peak *i* from the -CH_2- protons of the histidine R-group. The use of reductive amination to functionalize benzaldehyde containing block copolymers further highlights the use of this chemistry for post polymerization functionalization of polymers with varying architectures.

The resulting amino acid functional diblock copolymers, $\mathbf{P_{HIS}}$ and $\mathbf{P_{GLY}}$, are water soluble. The amino acid functional blocks are pH responsive, taking on different charged states in response to the pH of the solution. For $\mathbf{P_{HIS}}$, the histidine functional moiety can take on four charged states with three functional groups that can be protonated or deprotonated: the carboxylic acid (pKa 4.5), the imidazole (pKa 7) and the secondary amine (pKa 9).[44] $\mathbf{P_{GLY}}$ has the carboxylic acid and the secondary amine. The presence of both positive and negative charges, depending on the pH can affect the self-assembly of the polymers. The PNiPAm blocks are thermoresponsive, with that block taking on a hydrophobic character and making the polymers $\mathbf{P_{HIS}}$ and $\mathbf{P_{GLY}}$ amphiphilic with an increase in temperature. As PNiPAm is a thermoresponsive polymer, exhibiting a Lower Critical Solution Temperature (LCST) of 32 °C, the diblock copolymers $\mathbf{P_{HIS}}$ and $\mathbf{P_{GLY}}$ demonstrate reversible thermoresponsive self-assembly, illustrated in Scheme 2 for $\mathbf{P_{HIS}}$.

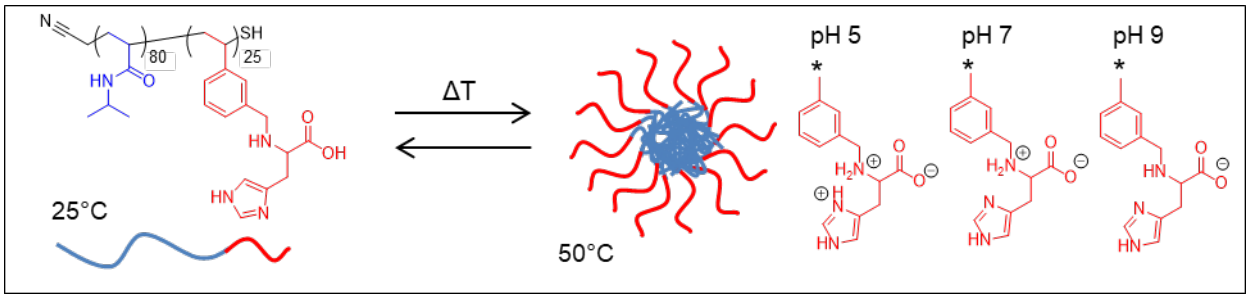

Scheme 2 The temperature-induced, reversible self-assembly of $\mathbf{P_{HIS}}$ with the charged states of the histidine moiety at pH 5, 7 and 9. Above 32 °C, the PNiPAm block takes on hydrophobic character to drive the self-assembly in water.

The temperature-induced self-assembly of these materials was investigated by ^{1}H NMR. $\mathbf{P_{HIS}}$ was dissolved into deuterated water and ^{1}H NMR spectra were taken at 25 °C, 50 °C and upon cooling again at 25 °C, illustrated in Figure 2. The bottom spectrum, (Figure 2a), is $\mathbf{P_{HIS}}$ at 25 °C. The peaks in this spectrum related to the histidine moieties (*c*, *d*, *e*, *f* and *g*) are broadened, likely due to the histidine moieties being shielded by the polymer self-associating via weak hydrogen bonding. Upon heating the sample to 50 °C, the peaks associated with the histidine moieties in the spectrum (Figure 2b) are much better resolved and are sharpened, indicating improved solubility. Additionally, the peaks associated with the PNiPAm have decreased in intensity relative to those of the sharpened histidine moieties. The PNiPAm peaks did not disappear and this could be due to the local increase in LCST of the PNiPAm blocks adjacent to the polar histidine blocks. Notably, the isopropyl proton (*b*), as well as the backbone signal is greatly reduced. These changes in the PNiPAm spectrum are

consistent with strong association of PNiPAm chains that occur during temperature-induced micellization. Upon cooling again to 25 °C, the signs of weak association of the histidine moieties return as the related peaks broaden and decrease in signal intensity. In addition, the backbone signal and the isopropyl signal increase in intensity once again indicating release from the thermally induced self-assembly. The pH of these solutions were not measured to avoid contamination of the deuterated solvent, however $\mathbf{P_{HIS}}$ dissolved in deionized water has a pH of ≈ 6.8, measured at a concentration of 1 mg/mL.

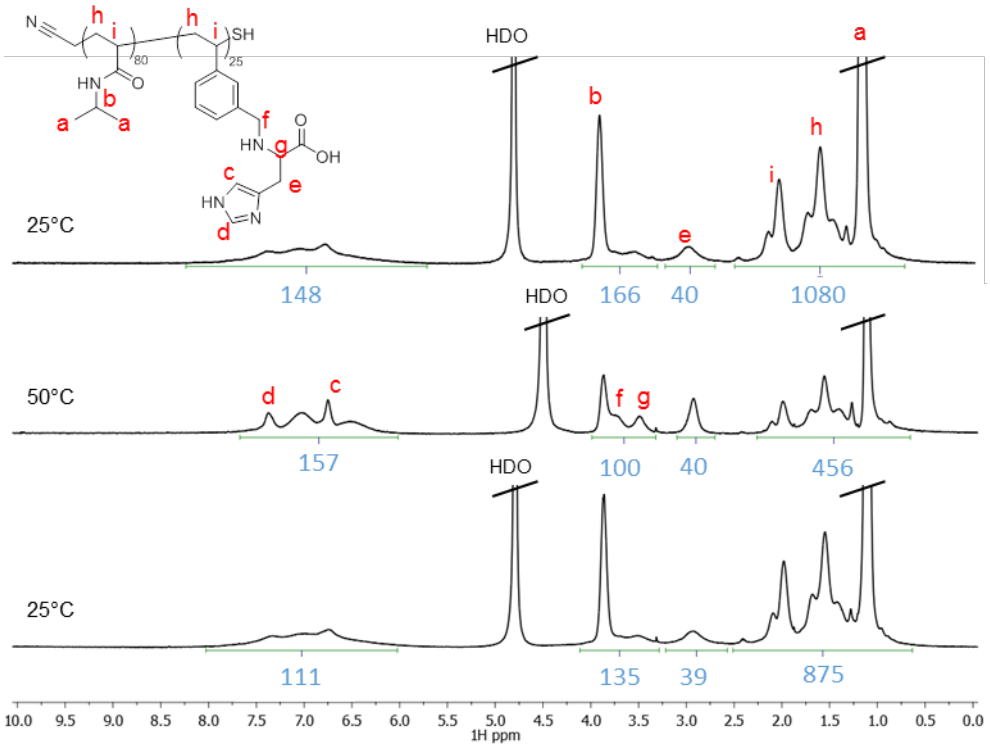

Fig. 2 The ^{1}H NMR spectra for $\mathbf{P_{HIS}}$ showing the reversible temperature-induced self-assembly of the polymer. At 25 °C, the peaks associated with the histidine moieties (*c*, *d*, *e*, *f* and *g*) are very broad, indicating some hydrogen bonding and some potential shielding from soluble PNiPAm blocks. At 50 °C, these peaks sharpen while the isopropyl protons (*a* and *b*) decrease in intensity as they move into the self-assembly.

The thermoresponsive behavior of $\mathbf{P_{GLY}}$ was similar to that of $\mathbf{P_{HIS}}$, observed by ^{1}H NMR in Figure S2. At 25 °C, the protons associated with the glycine functional block are broad. As the temperature is increased, the protons associated with the PNiPAm block decrease in intensity (these do not disappear completely which could be attributable to increased local LCST of the PNiPAm moieties adjacent to the polar glycine functional monomers) and the glycine (*e*) and benzylamine (*f*) peaks become a bit

sharper as the glycine groups are expressed in the corona of a sphere. Upon cooling, the PNiPAm peaks resume their intensity as the polymer solubilizes, and the glycine associated peaks become broader again as the polymer interacts weakly with itself. The change in relative intensities of the PNiPAm associated protons and the amino acid associated proton signals indicates a temperature-responsive self-assembly where the PNiPAm protons are shielded within a core above the LCST, with the amino acid functional blocks exposed to the exterior of the polymer self-assembly, in the corona. In addition, the ^{1}H NMR spectra confirm the presence of some self-assembly of $\mathbf{P_{HIS}}$ at 25 °C.

The self-assembly of $\mathbf{P_{HIS}}$ and $\mathbf{P_{GLY}}$ were also measured by dynamic light scattering (DLS). At pH values of 5, 7 and 9, the polymers undergo a reversible change in size upon an increase in temperature which is due to the temperature-induced amphiphilicity of the polymer as the PNiPAm block undergoes a coil to globule transition. The size of the polymer assemblies formed at 50 °C is dependent on the pH, which reflects the charges found on the amino acid functional block, shown in Figure S3 and S4 for $\mathbf{P_{HIS}}$ and $\mathbf{P_{GLY}}$, respectively. DLS also gives an indication of populations of self-assemblies, which in the context of highly functional polymers makes sense. These materials can hydrogen bond with themselves and with other polymer chains, as well as with the PNiPAm block which can also form strong hydrogen bonds. The presence of some self-assemblies that are ill defined and non-uniform at 25 °C measured by DLS is contrasted with really sharp, uniform and single sized populations at 50 °C. This supports the ^{1}H NMR measurements at 25 °C which show peak broadening that indicate some hydrogen bonding amongst these highly functional materials.

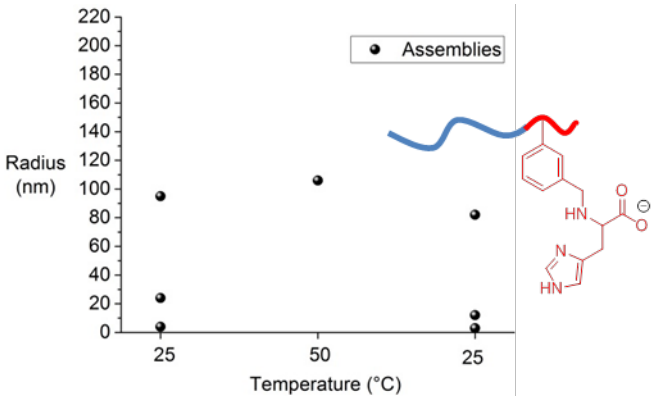

Fig. 3 Dynamic light scattering (DLS) was used to measure any polymer self-assemblies in solution (pH 9) above and below the LCST of PNiPAm to confirm the reversible self-assembly of $\mathbf{P_{HIS}}$ with a change in temperature. The charged state of the histidine moiety is shown. See SI for detailed DLS data.

At pH 9, the histidine block exhibits a negative charge. Figure 3 illustrates the temperature response of $\mathbf{P_{HIS}}$. At 25 °C, some polymer self-assemblies are detected by DLS and are likely due to some hydrogen bonding of the deprotonated amine and imidazole groups. Upon heating this sample to 50 °C, self-assemblies are again observed with a radius of 106 nm. Upon cooling, the block copolymers return to their multiple size populations indicating some self-association and hydrogen bonding that is not strong enough to stabilize the thermally induced self-assemblies.

The glycine functional polymer $\mathbf{P_{GLY}}$ exhibits very similar temperature-responsive behavior to $\mathbf{P_{HIS}}$ with the size of the temperature-induced assemblies dependent on the charged state of the glycine functional blocks, illustrated in Figure S4. At both pH 5 and 9, well defined micelles were observed upon heating the polymer solutions to 50 °C. The micelles formed at pH 5 were 160 nm while the micelles formed at pH 9 were smaller at 120 nm in radius. At pH 7, the $\mathbf{P_{GLY}}$ precipitated into stable assemblies visible with the naked eye, however did not precipitate out of solution. The increased aggregation size could be due to the zwitterionic nature of the glycine functional moiety at pH 7; the polar glycine moieties are charge neutral and this could be causing the aggregation of smaller self assemblies together, or the absence of charge repulsion of the glycine blocks could be increasing the size of the $\mathbf{P_{GLY}}$ assemblies relative to $\mathbf{P_{HIS}}$. The complete precipitation of the polymer was not observed as in the case with $\mathbf{P_{HIS}}$, and this could be due to the lack of the imidazole structure, which could also increase the hydrophobicity of the $\mathbf{P_{HIS}}$ block when it is not protonated.

After confirming the reversible temperature-induced self-assembly, the thermally induced $\mathbf{P_{HIS}}$ micelles were locked into place with Cu^{2+} ions, shown schematically in Scheme 3. No micelle locking was attempted at pH 7 due to the polymer precipitating out of solution. To lock the micelles using Cu^{2+} ions, the polymer solutions at pH 5 and 9 were heated to 50 °C with gentle stirring and held at 50 °C for five minutes to form micelles. To the heated polymer solution, 0.5 eq of Cu^{2+} ions was added relative to the histidine moieties. The sample was removed from heat and allowed to cool to room temperature while gently stirring. Once cooled, well-defined micelles were observed via DLS at pH 9, shown in Figure 4. The presence of single sized micelles at room temperature indicates that the thermally induced polymer self-assemblies were locked into place by metal ion coordination. The DLS measurements of these locked-self-assemblies was also confirmed by AFM images (Figure 4c), with the sizes of the self-assemblies obtained from AFM corresponding well to those given by the DLS measurements. The AFM measurements were also able to demonstrate an absence of self-assemblies where the DLS data showed ‘multiple populations’, shown in Figure 4b.

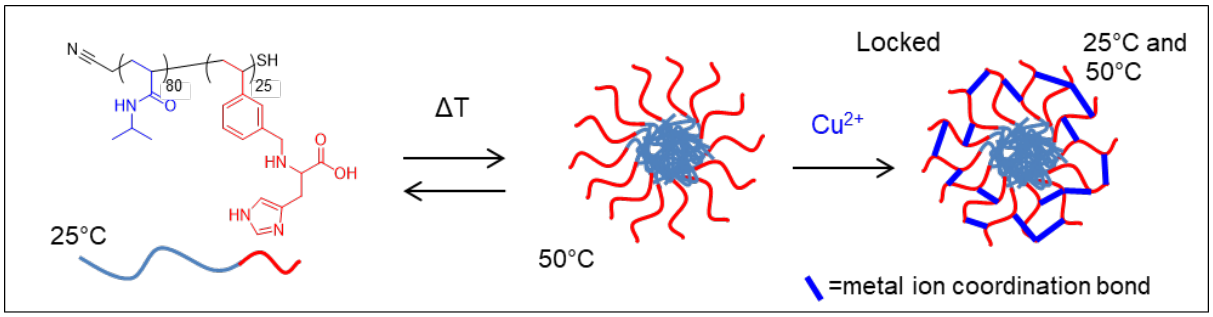

Scheme 3 The copper coordination crosslinking of the temperature-induced self-assemblies at 50 °C. Upon cooling, the Cu^{2+} coordination crosslinked micelles are present and stable.

The self-assemblies formed at pH 9 were very well defined and very stable in size after one month's time. Upon the addition of hydrochloric acid to these stable assemblies, the dissolution of the self-assemblies was observed. Additionally, the self-assemblies formed at pH 5 were not well-defined as a single sized population, indicating that the metal ion coordination is not as strong at pH 5, and the self-assemblies were even less well-defined after a few days. This indicates that the strength of this metal-ion coordination bond is dependent on the pH of the solution which is typical for metal-ion complexation with imidazoles. Messersmith and coworkers demonstrated that histidine metal ion coordination gels are dependent on the pH of the solution and that the ideal conditions for gelation was the deprotonation of an amine as well as a non-protonated imidazole, which occurred after adding 2 equivalents of NaOH to the histidine ligands.[32][45] In the case of our system, at pH 5 the imidazole and the secondary amine are protonated, and the protonation of the imidazole can interrupt the metal-ion coordination and weaken the interaction.At pH 9, stable micelles form when both the secondary amine and the imidazole are deprotonated. This indicates that this is the pH at which the metal ion coordination is strongest. Messersmith and coworkers were also able to show that gelation required the presence of an amine group to coordinate strongly with the metal ions. In the absence of the amine group, the metal ion coordination was present and visible with a change of colour, however, the bonds were not strong enough to form gels. They were however significant enough to affect the viscosity of a gel.[45] The stability of our metal ion locked micelles follows a similar trend, where stable micelles are held together when the pH is such that both the amine and the imidazole are deprotonated. In addition, while the micelles are temporarily stable at pH 5, they slowly return to unimeric form, indicating that the metal ion is coordinated, however the strength of the bond is not enough with the protonation of the coordinating groups.

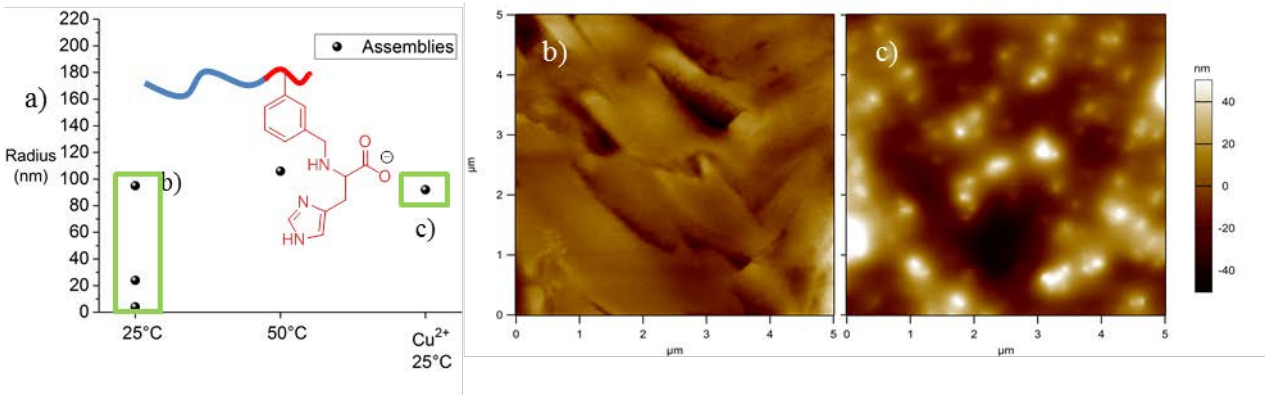

Fig. 4 The radii of the $\mathbf{P_{HIS}}$ self-assemblies at pH 9, measured by DLS, are shown in a). At 25 °C, $\mathbf{P_{HIS}}$ does not exhibit a single population by DLS, which is contrasted by the single population of 106 nm present upon heating the sample to 50 °C. AFM imaging of $\mathbf{P_{HIS}}$ on silicon at 25 °C shown in (b) shows a clear lack of polymer self-assemblies, confirming that the distribution of sizes measured by DLS are a result of $\mathbf{P_{HIS}}$ is self-associating via histidine groups as it is a functional material. After the addition of Cu^{2+} ions at 50 °C and cooling back to 25 °C, a single population of 96 nm polymer self-assemblies are measured by DLS. The presence of these stabilized micelles was confirmed by AFM imaging, shown in (c). Each AFM image displays a 5x5 um field with a 100 nm total z-range. See SI for detailed DLS data.

To ensure that Cu^{2+} ions did not contribute to the self-assembly of $\mathbf{P_{HIS}}$, it was introduced to the polymer sample at 25 °C as well as 50 °C. No uniform populations of micelles were found after the addition of Cu^{2+} to the polymer solution as shown in Figure 5. When the Cu^{2+} ions are added at 25 °C, they will interact with the histidine blocks randomly oriented in solution and might coordinate some chains together in this random orientation. When this sample is heated, precipitates form: histidine blocks are brought closer together as the PNiPAm takes on a hydrophobic character and becomes a globule. The presence of metal-ion coordination bonds during this self-assembly results in the formation of precipitates as the chains started to bond together when randomly oriented. This behavior is also observed in the glycine functional materials, shown in Figure S6.

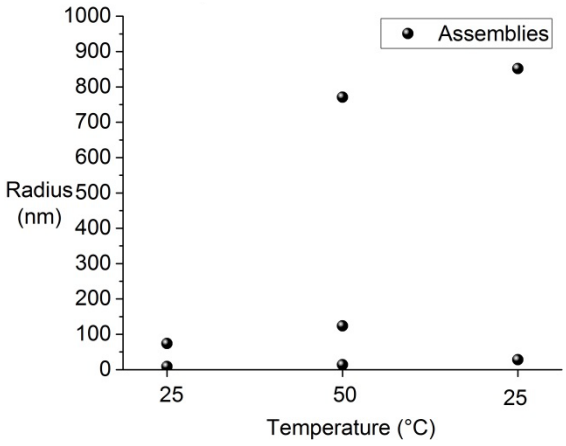

Fig. 5 DLS measurements of $\mathbf{P_{HIS}}$ in the presence of Cu^{2+} ions when they are added at 25 °C. After adding the Cu^{2+} ions, the solution was heated to 50 °C and cooled once again to 25 °C. A single population of self-assemblies was not observed, and thermally induced, reversible self-assembly was not observed. See SI for detailed DLS data.

To further investigate the stoichiometry of the Cu^{2+} to the histidine moieties in this metal ion coordination locking, the amount of copper added to the micelles was varied from His:Cu^{2+} 2:1 to 2:0.1, as outlined in Table S1. The only His:Cu^{2+} ratio that formed stable, single-sized self-assemblies was a 2:1 ratio. This is also consistent with other findings of histidine and amine containing metal ion coordination gels reported by Messersmith and coworkers.[32] The ratio of Cu^{2+} required for locked structures, in combination with the specific pH where locking occurs due to the deprotonation of the relevant coordination sites lends itself to the proposed coordination locking in Figure 6.

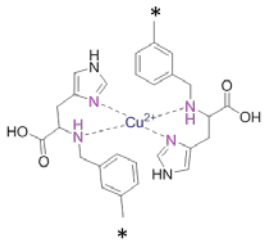

Fig. 6 The likely coordination mechanism of the $\mathbf{P_{HIS}}$ responsible for the locking of the micelles.

To ensure that the carboxylic acids are not contributing to the coordination of the metal-ion coordination proposed in Figure 6, the behavior of $\mathbf{P_{GLY}}$ in the presence of Cu^{2+} was investigated and compared to that of $\mathbf{P_{HIS}}$. At all pH values, no single population of $\mathbf{P_{GLY}}$ micelles was locked as $\mathbf{P_{HIS}}$ did at pH 9 with a 2:1 His:Cu^{2+} ratio. The addition of the Cu^{2+} at 50 °C resulted in a more turbid solution than when the Cu^{2+} was added at 25 °C. Importantly, the thermally induced self-assemblies

were not consistent or uniform upon the addition of Cu^{2+} ions which indicates that if any metal ion coordination is occurring in the $\mathbf{P_{GLY}}$ samples, these interactions are weak, lacking the strength to lock the $\mathbf{P_{GLY}}$ self-assembly corona to preserve the thermally induced assemblies. Figure S5 shows the DLS data of the $\mathbf{P_{GLY}}$ samples in the presence of copper, and AFM images confirming a lack of locked particles. The use of $\mathbf{P_{GLY}}$ as a control in this manner allows us to infer that if the carboxylic acids play any role in the metal ion coordination locking of the micelles, that role is miniscule.

Conclusion

In this work, we have synthesized amino acid functional block copolymers without protecting group chemistry, and investigated their self-assembly by DLS and ^{1}H NMR. We have demonstrated that the histidine and glycine blocks are expressed in the corona of the micelle upon thermally induced self-assembly upon heating to 50 ^{o}C. The introduction of Cu^{2+} ions at 50 ^{o}C can produce metal ion coordination locking of the histidine functional self-assemblies such that they do not disassociate upon cooling to 25 ^{o}C. The glycine functional micelles cannot be locked in this way by the addition of Cu^{2+} ions. The metal ion coordination bonds are a dynamic bond that can be employed for the reversible locking of polymer self-assemblies in the corona.

Acknowledgements

The authors would like to acknowledge financial support from the Victorian Endowment for Science, Knowledge, and Innovation (LAC), as well as the Commonwealth Scientific and Industrial Research Organization (CSIRO) Mineral Resources. The authors wish to thank the Particulate Fluids Processing Centre for providing research resources. The AFM imaging was done at the Materials Characterisation and Fabrication Platform (MCFP) at the University of Melbourne and the Victorian Node of the Australian National Fabrication Facility (ANFF).

References

[1] T.M. Allen, *Science* **2004**, *303*, 1818. doi:10.1126/science.1095833

[2] A.C. Rice-Ficht, A.M. Arenas-Gamboa, M.M. Kahl-McDonagh, T.A. Ficht, *Current Opinion in Microbiology* **2010**, *13*, 106. doi:10.1016/j.mib.2009.12.001

[3] D.W. Pack, A.S. Hoffman, S. Pun, P.S. Stayton, *Nature Reviews Drug Discovery* **2005**, *4*, 581.

doi:10.1038/nrd1775

[4] H. Mori, E. Takahashi, A. Ishizuki, K. Nakabayashi, *Macromolecules* **2013**, *46*, 6451. doi:10.1021/ma400596r

[5] H. Wang, K.R. Raghupathi, J. Zhuang, S. Thayumanavan, *ACS Macro Letters* **2015**, *4*, 422. doi:10.1021/acsmacrolett.5b00199

[6] A. Lu, P. Cotanda, J.P. Patterson, D. a. Longbottom, R.K. O'Reilly, *Chemical communications (Cambridge, England)* **2012**, *48*, 9699. doi:10.1039/C2CC35170F

[7] M.M. Zhu, F. Song, W.C. Nie, X.L. Wang, Y.Z. Wang, *Polymer (United Kingdom)* **2016**, *93*, 159. doi:10.1016/j.polymer.2016.04.035

[8] C. Chen, R.A.L. Wylie, D. Klinger, L.A. Connal, *Chemistry of Materials* **2017**, *29*, 1918. doi:10.1021/acs.chemmater.6b04700

[9] K. Kempe, R.A. Wylie, M.D. Dimitriou, H. Tran, R. Hoogenboom, U.S. Schubert, et al., *Journal of Polymer Science Part A: Polymer Chemistry* **2016**, *54*, 750. doi:10.1002/pola.27927

[10] J. Rodríguez-Hernández, F. Chécot, Y. Gnanou, S. Lecommandoux, *Progress in Polymer Science (Oxford)* **2005**, *30*, 691. doi:10.1016/j.progpolymsci.2005.04.002

[11] D. Klinger, M.J. Robb, J.M. Spruell, N.A. Lynd, C.J. Hawker, L.A. Connal, *Polymer Chemistry* **2013**, *4*, 5038. doi:10.1039/c3py00750b

[12] W. Zhao, H.T. Ta, C. Zhang, A.K. Whittaker, *Biomacromolecules* **2017**, *18*, 1145. doi:10.1021/acs.biomac.6b01788

[13] A.M. Nyström, J.W. Bartels, W. Du, K.L. Wooley, *Journal of Polymer Science Part A: Polymer Chemistry* **2009**, *47*, 1023. doi:10.1002/pola.23184

[14] E.D. Pressly, R.A. Pierce, L.A. Connal, C.J. Hawker, Y. Liu, *Bioconjugate Chemistry* **2013**, *24*, 196. doi:10.1021/bc300473x

[15] S. Binauld, M.H. Stenzel, *Chemical Communications* **2013**, *49*, 2082. doi:10.1039/c2cc36589h

[16] H. Lomas, I. Canton, S. MacNeil, J. Du, S.P. Armes, A.J. Ryan, et al., *Advanced Materials*

2007, *19*, 4238. doi:10.1002/adma.200700941

[17] R.K. O'Reilly, C.J. Hawker, K.L. Wooley, *Chemical Society Reviews* **2006**, *35*, 1068. doi:10.1039/b514858h

[18] D. Schmaljohann, *Advanced Drug Delivery Reviews* **2006**, *58*, 1655. doi:10.1016/j.addr.2006.09.020

[19] J. Du, R.K. O'Reilly, *Macromolecular Chemistry and Physics* **2010**, *211*, 1530. doi:10.1002/macp.201000022

[20] G. Ren, L. Wang, Q. Chen, Z. Xu, J. Xu, D. Sun, *Langmuir* **2017**, *33*, 3040. doi:10.1021/acs.langmuir.6b04546

[21] Y. Kim, M.H. Pourgholami, D.L. Morris, M.H. Stenzel, *Biomacromolecules* **2012**, *13*, 814. doi:10.1021/bm201730p

[22] K. Satoh, J.E. Poelma, L.M. Campos, B. Stahl, C.J. Hawker, *Polym Chem* **2012**, *3*, 1890. doi:10.1039/C1PY00484K

[23] B.S. Lokitz, A.J. Convertine, R.G. Ezell, A. Heidenreich, Y. Li, C.L. McCormick, *Macromolecules* **2006**, *39*, 8594. doi:10.1021/ma061672y

[24] J. Wang, A. de Keizer, R. Fokkink, Y. Yan, M.A. Cohen Stuart, J. van der Gucht, *The Journal of Physical Chemistry B* **2010**, *114*, 8313. doi:10.1021/jp1003209

[25] Y. Li, K. Xiao, J. Luo, W. Xiao, J.S. Lee, A.M. Gonik, et al., *Biomaterials* **2011**, *32*, 6633. doi:10.1016/j.biomaterials.2011.05.050

[26] A.B. Mabire, Q. Brouard, A. Pitto-Barry, R.J. Williams, H. Willcock, N. Kirby, et al., *Polym Chem* **2016**, *7*, 5943. doi:10.1039/C6PY01254J

[27] N.B. Pramanik, N.K. Singha, *RSC Adv* **2016**, *6*, 2455. doi:10.1039/C5RA22476D

[28] Y. Zhao, *Langmuir* **2016**, *32*, 5703. doi:10.1021/acs.langmuir.6b01162

[29] E.R.L. Brisson, Z. Xiao, L.A. Connal, *Australian Journal of Chemistry* **2016**, . doi:10.1071/CH16028

[30] S. Hederos, K.S. Broo, E. Jakobsson, G.J. Kleywegt, B. Mannervik, L. Baltzer, *Proceedings of the National Academy of Sciences* **2004**, *101*, 13163. doi:10.1073/pnas.0403045101

[31] K.J. Coyne, X.-X. Qin, H.J. Waite, *Science* **1997**, *277*, 1830. doi:10.1126/science.277.5333.1830

[32] D.E. Fullenkamp, L. He, D.G. Barrett, W.R. Burghardt, P.B. Messersmith, *Macromolecules* **2013**, *46*, 1167. doi:10.1021/ma301791n

[33] S.C. Grindy, R. Learsch, D. Mozhdehi, J. Cheng, D.G. Barrett, Z. Guan, et al., *Nature Materials* **2015**, *14*, 1210. doi:10.1038/nmat4401

[34] D. Mozhdehi, S. Ayala, O.R. Cromwell, Z. Guan, *Journal of the American Chemical Society* **2014**, *136*, 16128. doi:10.1021/ja5097094

[35] S. Tang, B.D. Olsen, *Macromolecules* **2016**, *49*, 9163. doi:10.1021/acs.macromol.6b01618

[36] P. Lundberg, N. a. Lynd, Y. Zhang, X. Zeng, D. V. Krogstad, T. Paffen, et al., *Soft Matter* **2012**, 82. doi:10.1039/c2sm26996a

[37] E.S. Lee, H.J. Shin, K. Na, Y.H. Bae, *Journal of Controlled Release* **2003**, *90*, 363. doi:10.1016/S0168-3659(03)00205-0

[38] J. Wang, M.A. Cohen Stuart, A.T.M. Marcelis, M. Colomb-Delsuc, S. Otto, J. van der Gucht, *Macromolecules* **2012**, *45*, 7179. doi:10.1021/ma301323z

[39] Z. Ge, S. Liu, *Macromolecular Rapid Communications* **2013**, *34*, 922. doi:10.1002/marc.201300072

[40] R. Ren, Y. Wang, W. Sun, *Reactive and Functional Polymers* **2016**, *106*, 57. doi:10.1016/j.reactfunctpolym.2016.07.018

[41] P.O. Shipman, C. Cui, P. Lupinska, R.A. Lalancette, J.B. Sheridan, F. Jäkle, *ACS Macro Letters* **2013**, *2*, 1056. doi:10.1021/mz400462h

[42] Y. Dai, X. Zhang, R. Zhuo, *RSC Adv* **2016**, *6*, 22964. doi:10.1039/C6RA02300B

[43] Y. Dai, X. Zhang, R. Zhuo, *Polymer International* **2016**, *65*, 691. doi:10.1002/pi.5118

[44] E.R.L. Brisson, Z. Xiao, L. Levin, G. V. Franks, L.A. Connal, *Polym Chem* **2016**, *7*, 1945. doi:10.1039/C5PY01915J

[45] S.C. Grindy, R. Learsch, D. Mozhdehi, J. Cheng, D.G. Barrett, Z.B. Guan, et al., *Nature Materials* **2015**, *14*, 1210. doi:10.1038/NMAT4401

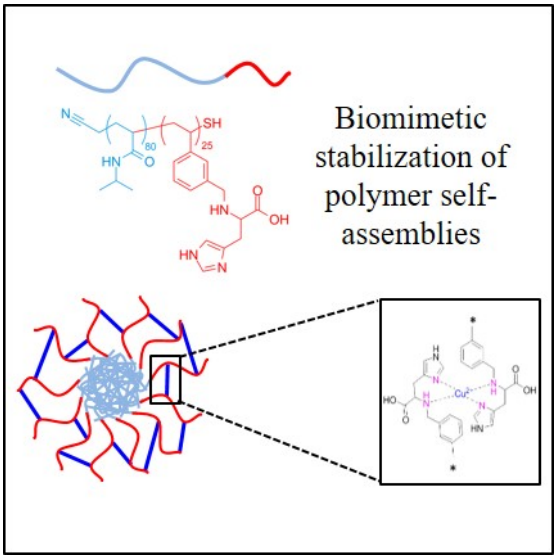

Graphical Abstract. Divalent copper ions are used to stabilize thermally induced self-assembled histidine functional polymer structures through metal ion coordination bonds.

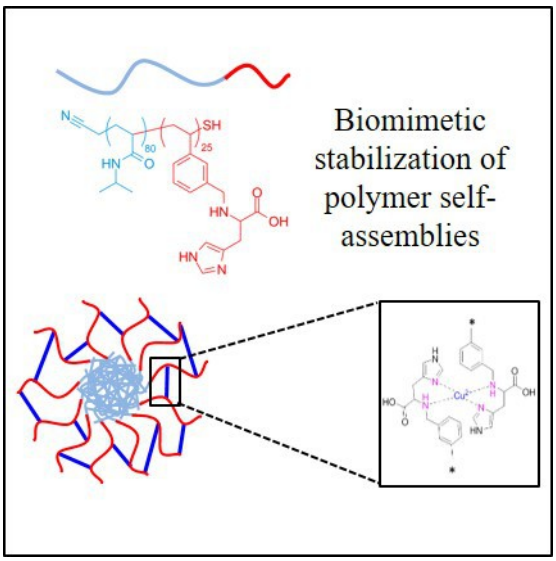

POLA_29351_toc attempt 2 (003).jpg

Author/s:
Brisson, ERL; Griffith, JC; Bhaskaran, A; Franks, G; Connal, LA

Title:
Temperature-induced self-assembly and metal-ion stabilization of histidine functional block copolymers

Date:
2019-09-15

Citation:
Brisson, E. R. L., Griffith, J. C., Bhaskaran, A., Franks, G. & Connal, L. A. (2019). Temperature-induced self-assembly and metal-ion stabilization of histidine functional block copolymers. Journal of Polymer Science Part A: Polymer Chemistry, 57 (18), pp.1964-1973. https://doi.org/10.1002/pola.29351.